FLORAL STRUCTURE AND DYNAMICS OF NECTAR PRODUCTION IN *ECHINACEA PALLIDA* VAR. *ANGUSTIFOLIA* (ASTERACEAE)

Tyler J. Wist and Arthur R. Davis[1]

Department of Biology, University of Saskatchewan, 112 Science Place, Saskatoon, Saskatchewan S7N 5E2, Canada

The reproductive structure of the disk florets of *Echinacea pallida* var. *angustifolia* (Asteraceae) in relation to insect pollination was investigated using light, fluorescence, and scanning electron microscopy. The study of this self-incompatible species emphasized pollen production, pollen-stigma interactions, transmitting tissue, and vasculature within the style. Nectary structure and nectar production dynamics were also examined. Produced in the fused anther tubes, the trinucleate pollen with yellow pollenkitt was plentiful per floret, yielding a pollen : ovule ratio of 24,130. Encircling the style base at the ovary summit, the floral nectary possessed modified stomata whose pores, as well as nonstomatal gaps in the epidermis, provided apoplastic pathways for nectar escape and reabsorption. Phloem alone supplied the gland interior, the sieve element–companion cell complexes reaching up to the nectary epidermis. Nectar was hexose dominant, its volume and nectar-sugar quantity per floret peaking on the afternoon of the first day of anthesis until the morning of the second day. Nectar production only occurred in half of the florets for 3 d, rarely for 5 d. Potential honey production from fields of this species was estimated at 2.1–11.9 kg/ha.

Keywords: floral nectar, nectary, pollen-stigma interactions, pollination, style.

Introduction

Based on molecular data, *Echinacea angustifolia* has recently been reclassified as a subspecies of *Echinacea pallida* (Binns et al. 2000). *Echinacea pallida* var. *angustifolia* (narrow-leaved purple coneflower) is a native species on the North American prairies, where it is also grown as a specialty crop on a limited acreage to supply the demand for herbal preparations from its various organs. The primary commodity of *E. pallida* var. *angustifolia* is its thick tap root, but secondary products include aerial stems and achenes that may be brought to market during the years before root harvest. The species is self incompatible (McGregor 1968) and hence reliant on cross-pollination for fruit set.

The inflorescences of several *Echinacea* spp. were studied in detail and included measurements of many floral organs of *E. pallida* var. *angustifolia* (McGregor 1968). Disk florets immediately inward from the capitulum's showy pink ray florets (fig. 1A) open first and are protandrous (Wagenius 2004). However, during the pistillate phase of the disk florets, when most self pollen has been gathered by insects and stigmas are receptive to outcross pollen, nectar is the primary reward offered to foraging insects. No studies of nectar production throughout flowering exist for this species, yet such an investigation is essential to understanding the attractiveness of the self-incompatible disk florets to insect foragers.

Although inflorescences are visited by honey bees (*Apis mellifera* L.) for nectar and pollen, there are no ratings currently available for *Echinacea* spp. as honey plants (Crane et al. 1984). Introducing honeybee colonies to fields of *E. pallida* var. *angustifolia* could fulfill the crop's cross-pollination requirements and provide a prolonged source of floral nectar

[1] Author for correspondence; e-mail: art.davis@usask.ca.

for honey production. The potential therefore exists to develop honey as a product from *Echinacea* fields while providing an adequate supply of bees as cross-pollinators to ensure the production of high-quality achenes.

Accordingly, the objectives of this study of *E. pallida* var. *angustifolia* are fourfold. For the first time, (1) structural reproductive features of the self-incompatible disk florets as they relate to insect pollination are examined; (2) the interaction of pollen grains with the stigma and pollen-tube growth through the style are investigated; (3) the production of nectar by disk florets is followed from anthesis to senescence, in order to understand periodicity of disk-floret attractiveness to insects; and (4) the potential for honey production is estimated.

Material and Methods

Plants and Field Sites

Mature plants of *Echinacea pallida* var. *angustifolia* (DC) Cronq. were sampled at three field sites in the summers of 2004 and 2005. Chief Whitecap Park of the Meewasin Valley Authority is located near the South Saskatchewan River on the northeastern side of Saskatoon. This field site, once a cultivated plot of this species, still contained thousands of plants in a nonmanaged setting.

The second site was an organic farm located 7 km west of Saskatoon on Valley Road, on the west bank of the South Saskatchewan River near Poplar Bluffs Canoe Launch. In 2004, the plants were in their fifth year of growth, and many had attained a bushy habit with numerous inflorescences per plant.

Eight plants of *E. pallida* var. *angustifolia* were transplanted from the first site into a garden plot north of the W. P. Thompson Building, University of Saskatchewan, in spring 2003. In 2004 and 2005, the number of *E. pallida* var. *angustifolia* plants at
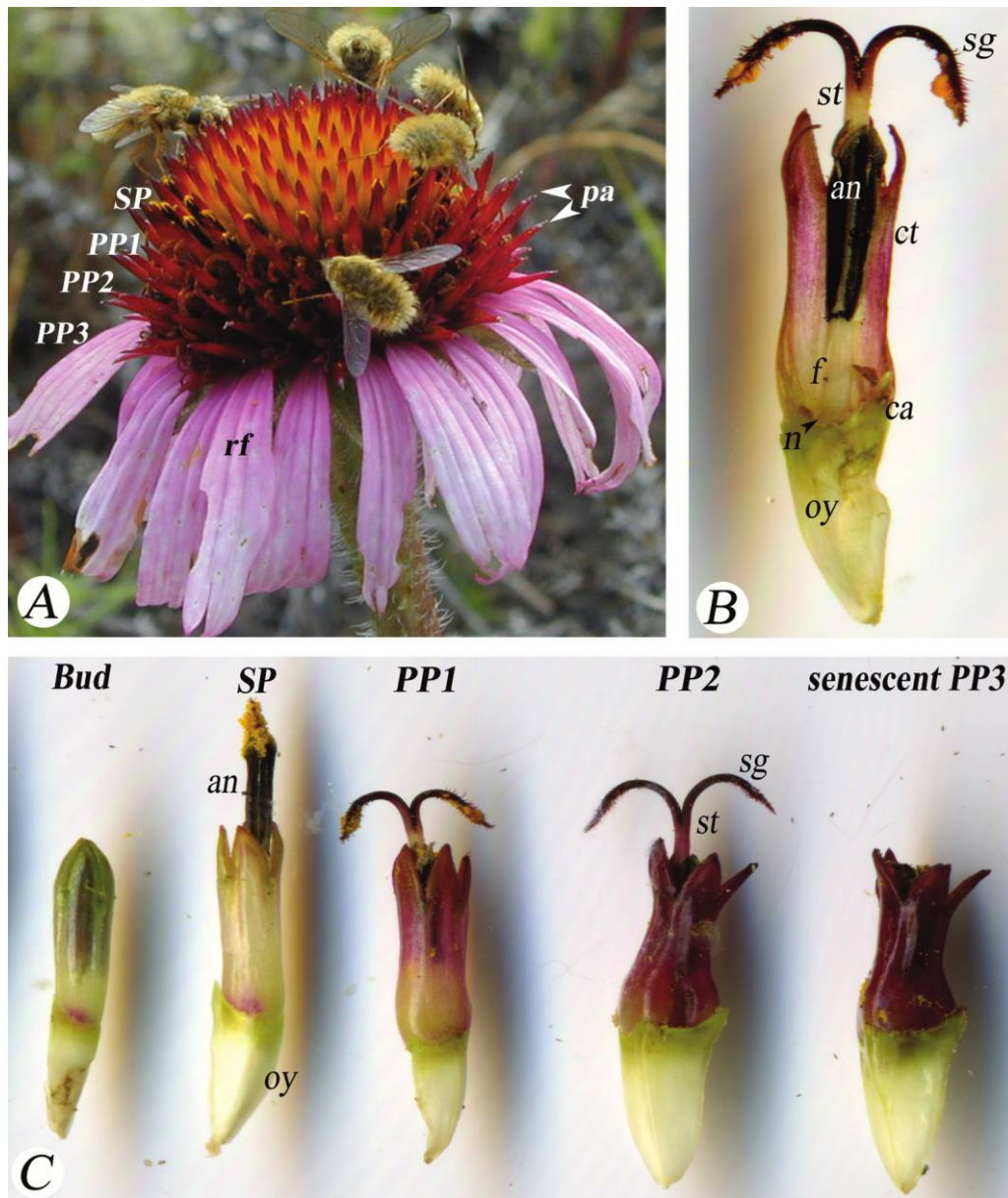
Fig. 1 *A*, Inflorescence of *Echinacea pallida* var. *angustifolia* visited by bee flies (*Systoechus vulgaris*), showing disk florets of the staminate phase (*SP*); first day (*PP1*), second day (*PP2*), and third day (*PP3*) of the pistillate phase; ray florets (*rf*); and paleae (*pa*). *B*, Disk floret dissected to show the adnate filament (*f*), anthers (*an*), calyx (*ca*), nectary (*n*), ovary (*oy*), stigma lobes (*sg*), style (*st*), and tubular corolla (*ct*). *C*, Disk florets from five phases: mature bud, staminate phase (*SP*); first day (*PP1*), second day (*PP2*), and third day (*PP3*) of the pistillate phase; anther (*an*); ovary (*oy*); stigma lobes (*sg*); style (*st*).

this third field site increased naturally. Voucher plants were placed in the W. P. Fraser Herbarium (SASK). For comparative purposes, some observations were also made from disk florets of *Echinacea purpurea* L. (Moench) growing on a greenhouse bench (Wist and Davis 2006).

Disk-Floret Structure

SEM. For morphological study of overall structure, disk florets of the mature bud, the dehiscent staminate (SP), the first-day pistillate (PP1) stage, and the senescent (PP3) stage (fig.

1*A*, 1*C*) were harvested from *E. pallida* var. *angustifolia* plants at the first and third field sites and processed for SEM. Inflorescences were bagged before the first whorl of disk florets reached anthesis in order to prevent potential insect damage to the florets. Florets were removed from inflorescences before fixation in 2% glutaraldehyde (GA) in 25 mM Na phosphate buffer, pH 6.8, for 0.5 h. After rinsing three times with phosphate buffer, tissues were postfixed for 2 h in 1% OsO_4 in buffer. Three rinses each of buffer and distilled water were followed by dehydration in a graded series of acetone. Tissues were critical-point dried with liquid CO_2 (Polaron Instruments,

Watford), mounted on aluminum stubs with two-sided tape, coated with gold (Edwards S150B Sputter Coater, Wilmington, MA), observed with a Philips SEM 505 (Eindhoven, Netherlands) at 30 kV, and photographed with Polaroid 665 positive/negative film. Negatives and positives were scanned (Epson 3200 Photo, Epson CX3810, Toronto, Ontario), and images were labeled and arranged using Adobe Photoshop 7.0.

For detailed studies of nectary morphology, nectaries from disk florets in four distinct phenological stages (mature bud, SP, PP1, and senescent PP3; fig. 1C) were removed from mature inflorescences of two plants and processed for SEM. In some samples, exterior floral organs were first removed to expose the nectary, which remained on the inferior ovary (fig. 1B). Nectary dimensions and the number and developmental stage of the modified stomata on the nectary surface were compared between floral stages.

LM. Disk florets of two distinct developmental stages (late staminate phase SP 24 h after anthesis, when the pollen mass remained on the prereceptive stigma lobes of the pollen presenter, and early PP2 48 h postanthesis, with stigma lobes fully bifurcated and receptive) were harvested from the same inflorescence and dissected to the nectary atop a cross-sectioned ovary. Tissues were fixed in 1.5% GA in 25 mM Na phosphate buffer, pH 6.8, for 0.5 h at room temperature before transferring to 3% GA in buffer for 2 h. On ice, samples were rinsed with buffer for 1–12 h, postfixed overnight with 1% OsO_4, then rinsed with distilled water before dehydration in an ethanol series. A gradual substitution of ethanol by propylene oxide preceded sample infiltration and embedding in Araldite 502 resin at 60°C for 24 h. Semithin sections (2 μm) of floral nectaries were then cut on a Reichert OMU3 (Tucson, AZ) ultramicrotome, floated on distilled water, briefly flamed to heat-fix them to microscope slides, stained with toluidine blue (O'Brien and McCully 1981), rinsed of excess stain, and then mounted in immersion oil under coverslips. Sections were examined with a Zeiss Universal (Thornwood, NY) microscope, photographed with Fujifilm Superia Iso 100 film, and arranged using Adobe Photoshop 7.0. Fresh tissues, including the floral nectary, were also examined after staining with I_2KI for starch (Johansen 1940) and pollen grains stained with acetocarmine (Belling 1921).

Fluorescence microscopy. The occurrence of phloem in floral organs such as the nectary and style was investigated using epifluorescence optics. Intact florets above the ovary were stained overnight at room temperature in 0.1% aniline blue in 0.1 M K_3PO_4, which binds to callose (β-1,3-glucan) of sieve-tube elements (Martin 1959). The whole mount was then slightly compressed with a coverslip on a microscope slide.

Determination of pollen quantity per floret. For *E. purpurea*, the average number of pollen grains per disk floret was determined by counting the total grains from all five anthers within one indehiscent but otherwise mature anther tube from each of five plants. Four additional disk florets from the same capitulum of one of the same plants were randomly selected and their pollen contents counted. The entire anther tube was dissected from a disk floret before dehiscence, ensuring that all grains produced were still present, and then split open with a razor blade to release pollen into a drop of water on a microscope slide. The opened anther tube was transferred through five subsequent water droplets until all pollen was removed

from anthers and suspended in water. Coverslips were placed over the droplets and sealed with nail polish to prevent evaporation. All grains from each anther tube were counted at ×100 using a compound microscope (Olympus, Center Valley, PA).

For *E. pallida* var. *angustifolia*, this same method was employed for the first disk floret sampled. However, owing to the larger quantity of pollen produced in this species, mature buds with their corolla tips closed were subsampled for their pollen as follows. Anthers were carefully stripped longitudinally from their fused tubes and transferred to an Eppendorf centrifuge tube (1.5 mL) containing 750 μL distilled water. Pollen was dislodged and suspended by vortexing (Mini Vortexer, VWR, West Chester, PA) for 2 min at top speed. After 1 h, each centrifuge tube was vortexed again for 1 min to eliminate pollen clumping, providing an even distribution of solitary grains for counting when 75 μL of the suspension was applied by pipette to a microscope slide. One more disk floret from each of three plants, plus five florets randomly chosen from the same row of the capitulum of another plant, were also subsampled.

Nectar dynamics throughout floret phenology. To estimate the quantity of nectar sugar per stage of floret phenology encountered by potential pollinators on the capitulum of *E. pallida* var. *angustifolia*, inflorescences were bagged (2.5 mesh/mm) to exclude nectar loss to insects. Sampling of nectar was attempted from disk florets during three intervals (morning: 0900–1100; midday: 1101–1400; afternoon: 1401–1900) for each phenological stage (SP, PP1–PP4). Stage PP4 is a floret like PP2 in figure 1C but not cross-pollinated and hence not yet senescent, by the fourth day of its pistillate phase. Disk florets were sampled for nectar in the field but not within 24 h of precipitation, to avoid any nectar dilution by rain. An individual floret was sampled only once, rather than on repeated occasions, and a range of 5–15 disk florets per phenological stage was assayed per inflorescence. Nectar was harvested from four inflorescences of different plants at each of sites 1 and 2 in 2004. The majority of nectar sampling, however, was conducted on 12 plants and 14 inflorescences at site 3 in 2004 and 2005.

Nectar volume. A 0.2-μL microcapillary tube (Drummond Microcaps) of common bore was inserted to the corolla base, and the volume of withdrawn nectar was calculated from the height of the nectar column.

Nectar solute concentration. Following volume measurement, nectar was expelled onto the prismatic surface of a handheld refractometer (0%–50%, 40%–85%; Bellingham and Stanley, Tunbridge Wells, Kent) modified by the manufacturer for small quantities of fluid. Approximately 90% of samples yielded a reading. These nectar solute concentrations based on mass (NCM) were corrected to 20.0°C (manufacturer's manual).

Nectar-sugar quantity per disk floret. Corrected nectar solute concentrations (%NCM) were converted to micrograms solute per microliter nectar (NCV) using the equation of Búrquez and Corbet (1991). The nectar-sugar quantity per disk floret was estimated as the product of nectar volume and NCV.

Nectar-carbohydrate composition. For three plants, nectar was collected separately for each of three phenological stages (SP, PP1, PP2) by pooling nectar from several florets per whorl into a 1-μL microcapillary before expulsion onto a filter-paper wick (McKenna and Thomson 1988). Nectar volumes in PP3 and PP4 stage florets were insufficient for carbohydrate analysis. Sampling from these three stages of florets was achievable from

consecutive whorls within the same inflorescence, thereby allowing comparison of nectar-carbohydrate composition within a genotype. Air-dried wicks were stored individually in labeled envelopes at room temperature. Wicks were later eluted individually in 2 mL Eppendorf tubes containing 150–1000 μL of pure distilled water, depending on the dilution rate required to allow carbohydrate peaks to fall within the range of standard curves ($r = 0.99$ for each carbohydrate) created for each major nectar sugar (glucose, fructose, sucrose; 5–200 ppm). After filtering, 50 μL of each sample were analyzed in duplicate using a Waters HPLC system, as described in Davis et al. (1998).

Results

Inflorescences and Ray Florets

Typically, in its first year of growth, each plant of *Echinacea pallida* var. *angustifolia* begins as a basal rosette of leaves that bolts in late spring or early summer to produce a single capitulum. However, some plants do not produce an inflorescence in their first year of growth. By the third through fifth years of growth, the plant often takes on a bushy appearance and can produce multiple inflorescences from shoots derived from lateral rhizomes. The root and rhizome are perennial and increase in size during each growing season, sending out new shoots and leaves each spring.

The first inflorescence to reach anthesis was borne terminally on the central stalk (peduncle). Other inflorescences may develop from axillary buds on the shoot, depending on plant age. Surrounding the inflorescence were green, imbricate, involucral bracts covered in trichomes visible beneath the ray florets (fig. 1A). The cone-shaped capitulum enters anthesis with maturation of the outer single whorl of sterile, ligulate (ray) florets, which surround multiple whorls of disk florets (fig. 1A). Corollas of ray florets comprised three petals in the ligule, lacked "nectar-guide" patterns, and ranged in color from purplish pink to deep purple; most drooped when mature. Ray florets were sterile, lacking an androecium and a full gynoecium, except for an ovary. In rare cases, ray florets possessed a stigma and style, but it was not determined whether these florets produced viable achenes. In all other ray florets, the ovary wall of the achene hardened but failed to yield a viable fruit due to the incomplete gynoecium.

Phenology of Disk Floret

After expansion and pigmentation of the corolla of the ray florets (fig. 1A) that coincided with lateral expansion of the inflorescence, the protandrous disk florets developed centripetally and sequentially, in whorls. The mean number of disk florets per capitulum was 202 ± 3.7 (SE; $n = 280$ plants sampled at the three field sites over two seasons). One whorl of mature buds reached anthesis per day by entering into the staminate stage (SP) upon anther dehiscence (fig. 1A, 1C). Anthers fused along their length protruded beyond the corolla tube in the early morning of the staminate phase, and a yellow pollen mass (fig. 1C, SP) typically was presented by 0900, depending on climate. Pollen release often coincided with incidence of the morning sun on the anthers; pollen was not presented during rainy periods. On the second day of flower-

ing, the elongating style extended through the anther tube and pollen mass before the two stigma lobes reflexed; this initial pistillate phase was designated PP1 (fig. 1A, 1C). Stage PP2 (fig. 1C) marked the second day of stigmatic receptivity. Disk florets remained in the receptive pistillate stage for up to 8 d (e.g., *PP2* in fig. 1C), until anthesis was complete, or until cross-pollination occurred, at which point the stigma lobes and style shrivelled at senescence and withdrew into the corolla tube (senescent *PP3* in fig. 1C).

Perianth Morphology of Disk Florets

Each disk floret of *E. pallida* var. *angustifolia* was subtended by a bract (palea) (fig. 1A) that gave the capitulum's center an echinate appearance. Each disk floret was perfect and epigynous (fig. 1B), with the inferior ovary embedded in the cone-shaped inflorescence.

Sepals of the fused calyx (pappus) were highly reduced and existed only as a fringe of green tissue at the ovary summit, surrounding the corolla base (fig. 1B, 1C; fig. 2E, 2F). The pappus had unevenly serrate margins (fig. 2F) with a prominent extension on the side adjacent to the palea (fig. 2E, 2F, bottom).

Corolla color varied from green at anthesis (fig. 1C, left) to reddish purple in the pistillate phase (fig. 1C, right). The campanulate corolla of five petals (fig. 2B, 2D) initially had a narrow base (figs. 1C, left, 2E) that gradually enlarged to a bulge (fig. 1C, right), thus serving as a nectar reservoir. At the corolla apex, petal lobes were distinct (fig. 1C; 2B, 2D). Patches of short, unicellular trichomes were often found on the lobe margins (fig. 2A). However, uniseriate trichomes occurred infrequently and at random intervals on the outer corolla surface (fig. 2B, 2D).

Androecium of Disk Florets

The androecium was composed of five synantherous stamens. The stamens were epipetalous, their filaments adnate to the petals basally (figs. 1B, 2E, 4A). Anthers were coalescent and fused into a tube (fig. 2D), the filaments remaining free (fig. 2E). Each mature anther contained two elongated pollen sacs (microsporangia) that released pollen grains by inward longitudinal dehiscence up to the bases of the anther's apical extensions (fig. 2C). Pollen aggregation within pollen sacs was evident when anther walls were removed, leaving the grains molded into the shape of the pollen sacs (fig. 2G). Pollen presentation was secondary, with the microgametophytes released inside the tube being swept out and presented on the top of the anther tube (SP in fig. 1C) by the extrusion of the stigma (fig. 2D) and contraction of the filaments (PP1 in fig. 1C), which was evident when gentle pressure was applied to filaments with a glass micropipette. Each morning between sunrise and 0900, a new whorl of disk florets opened into the indehiscent staminate stage (SPi). The florets released their pollen from the top of the tube between 0900 and 1100, weather permitting, as they entered the dehiscent staminate phase (SPd). By 2130, florets had passed through the staminate phase and entered the receptive pistillate phase (PP1) characterized by reflexed stigma lobes.

Pollen grains of *E. pallida* var. *angustifolia* were yellow at dehiscence (fig. 1A–1C) and had a tendency to clump together due to the presence of yellow droplets of oily pollenkitt ad-
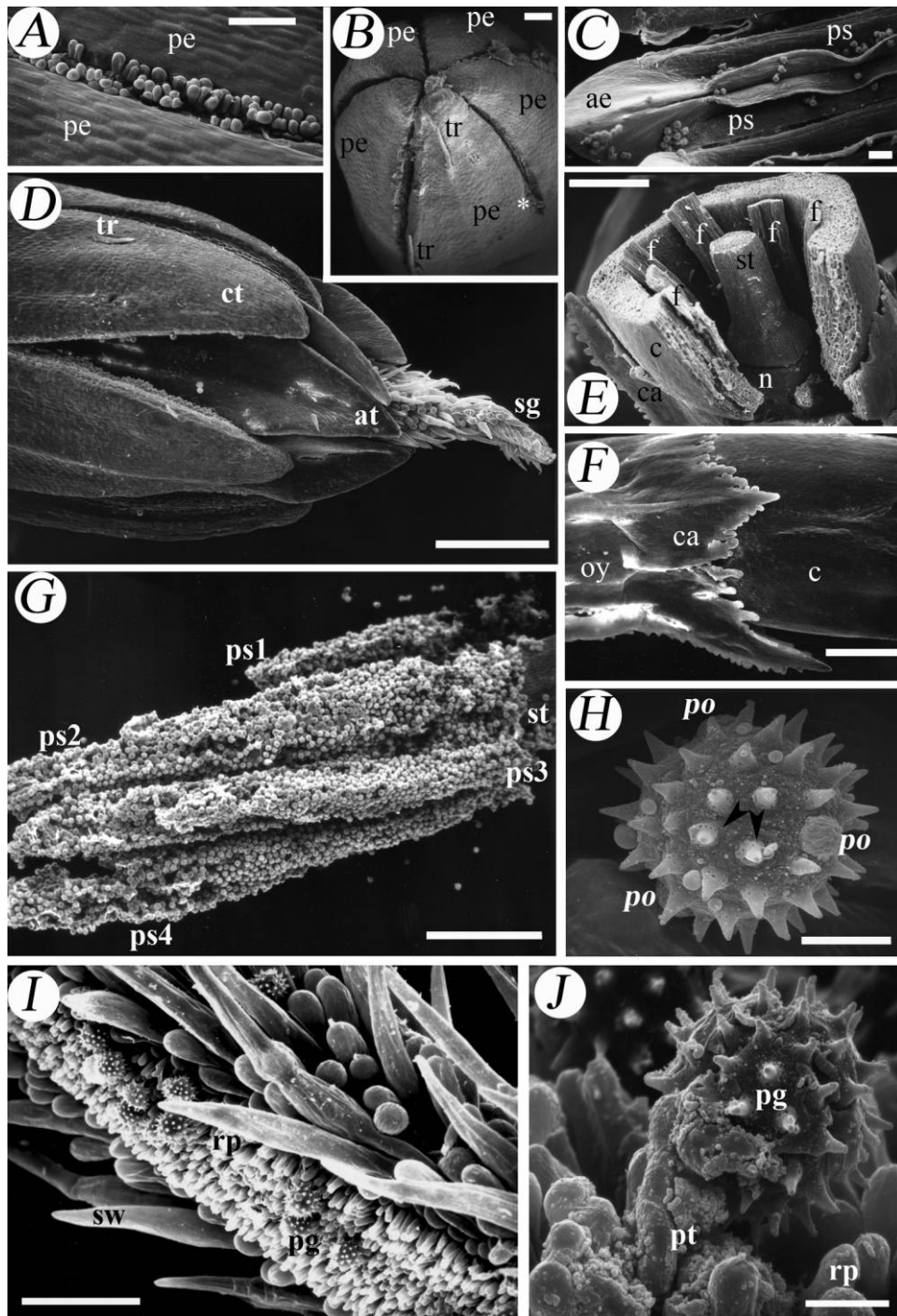
Fig. 2 SEMs of disk florets. *A*, Papillae on the base of the inner, unfused margins below the tips of two adjacent petals (*pe*) of the fused corolla tube, corresponding to the asterisk in *B*. Scale bar = 0.1 mm. *B*, Bud stage, showing fusion of five petals (*pe*) into a tube and the papillate inner margin (asterisk) and several two-celled, uniseriate trichomes (*tr*) on outer petal surface. Scale bar = 0.1 mm. *C*, Inner surface of an anther with the sterile apical extension (*ae*) and nearly empty pollen sacs (*ps*). Scale bar = 0.1 mm. *D*, Staminate-phase floret. Corolla tube (*ct*) with elongated trichome (*tr*), anther tube (*at*), and emergent stigma (*sg*) acting as pollen presenter. Scale bar = 0.5 mm. *E*, Transverse section through corolla base (*c*), indicating arrangement of staminal filaments (*f*), style (*st*), and nectary (*n*). Calyx indicated by *ca*. Scale bar = 0.5 mm. *F*, Insertion of calyx (*ca*) at junction of corolla (*c*) and ovary (*oy*). Scale bar = 0.5 mm. *G*, Inner surface of anther tube, showing abundance of pollen within pollen sacs (*ps*). Pollen grains from two anthers are visible (*ps1*, *ps2* represent one anther; *ps3*, *ps4* represent the second anther). Style indicated by *st*. Scale bar = 0.5 mm. *H*, Tricolporate pollen grain with pores (*po*) and microperforations of the spines (arrowheads). Scale bar = 10 μm. *I*, Self pollen grains (*pg*) on receptive surface of a stigma at the zone where receptive papillae (*rp*) meet sweeping trichomes (*sw*). Scale bar = 0.1 mm. *J*, Oily pollenkitt on surface of pollen grain (*pg*) with tube (*pt*) penetrating the stigma surface. Receptive papilla indicated by *rp*. Scale bar = 10 μm.

hering to the grain exterior (figs. 2J, 3A). Grains were echinate with microperforated spines and tricolporate with three typically prominent apertures (fig. 2H).

Pollen grains of *E. pallida* var. *angustifolia* and also *Echinacea purpurea* (Wist 2005) were trinucleate at the time of anther dehiscence (fig. 3A). One round tube (vegetative cell) nucleus and two laminar sperm cells—often parallel to each other—were visible within the cytoplasm.

In *E. purpurea*, the average quantity of pollen grains from five indehiscent anther tubes randomly selected within one capitulum was 9296 ± 666 (SE). Total pollen from single disk florets from four other plants ranged from 7464 to 14,231 grains. Thus, with a solitary ovule available per floret (fig. 4A), the pollen : ovule ratio was 10,414 ± 2239 (SE; *n* = 5 plants).

In *E. pallida* var. *angustifolia*, five disk florets within the same row of an inflorescence averaged 26,580 ± 591 (SE) pollen grains. From the other four plants sampled, total pollen per disk floret varied from 17,910 to 29,464 grains, yielding a pollen : ovule ratio of 24,131 ± 4770 (SE; *n* = 5).

Gynoecium of Disk Florets

The gynoecium consisted of one bilobed stigma, one style, and one inferior ovary (fig. 1B). Within the unilocular ovary was one ovule (fig. 4A). The stigma lobes were equal in length (fig. 1B) and had long sweeping trichomes (fig. 2D, 2I; fig. 4I) on the nonreceptive abaxial surface that transported pollen grains from the interior of the anther tube and presented them above the anther tips (SP in fig. 1C). The two receptive surfaces of the stigma abutted and covered each other at this time, preventing the majority of self pollen from contacting them. Separation of the stigmatic lobes (fig. 1B; PP1 in fig. 1C) signified onset of the pistillate phase. The receptive adaxial surface of the stigma was covered with papillae (fig. 2I, 2J; fig. 4I) that lacked any exudate (i.e., a dry-type stigma). If the stigma was not cross-pollinated after several days of receptivity, the stigma lobes reflexed further to potentially bring their receptive adaxial surfaces into contact with self pollen grains remaining on the anthers.

One vascular bundle containing both xylem and phloem entered each stigmatic lobe (fig. 4I) after traveling up either side of the style (fig. 3B) from its base (fig. 3D, 3E), often with several isolated sieve tubes found several cell layers away from the phloem of the two wide vascular bundles (fig. 3B, 3D). These isolated phloem traces were also found in *E. purpurea* (fig. 3C). In the center of the style was the transmitting tract for conducting pollen tubes to the ovule (fig. 3C, 3D). The center of the transmitting tract was hollow near the base of the style in *E. pallida* var. *angustifolia* (fig. 3D; fig. 4G, 4H, 4J) but lacked this hollow center in the majority of the upper portion of the style in both *E. pallida* var. *angustifolia* and *E. purpurea* (fig. 3C). A dense-staining intercellular matrix occurred among cells of the transmitting tract (fig. 3C, 3D). The transmitting tract extended into each stigma lobe and was found directly beneath the papillae of the receptive surface, where it eventually declined to one cell layer at the stigma lobe tip from a dense layer 4–5 cells in thickness in the rest of the lobe (fig. 4I). Each compatible pollen grain on the receptive surface could produce a single pollen tube (fig. 2J) that passed between the papillae and penetrated the transmitting tissue beneath.

Nectary Anatomy

The yellowish nectary of the disk florets takes its final cup-shaped and pentamerous form (fig. 5A) from pressure exerted on its inner surface during its formation by the style base and the bases of the five fused petals from outside it. Nectary diameter increased throughout the disk-floret phenology by means of senescent florets that are slightly less than twice the width of mature buds (table 1). Nectary height was less variable across stages, with mean sizes ranging from 164 to 229 μm (table 1).

Modified stomata occurred on the nectary surface and were the most likely route for nectar escape. However, nonstomatal openings that may also serve as sites of nectar escape were observed in the epidermis (fig. 5C, 5E). Most stomata occurred singly, but there were infrequent exceptions (figs. 3F, 5F) where guard mother cells of adjacent stomata may have arisen from the same cell division. Both guard cells and nonspecialized epidermal cells had a ridged appearance owing to the cuticular ridges that on the guard cells ran circumferentially along each side of the pore (fig. 5C, 5D, 5F). Nectaries had an average of 35–41 modified stomata (table 1), with the majority located on the upper rim (fig. 3E; fig. 4D, 4E, 4G; fig. 5A) but with several occurring on the lower nectary walls (figs. 3E, 5B). Nectaries of mature buds had a greater proportion of immature stomata (21%; table 1), where the outer cuticle spanning the circumferential ledges had not yet torn to reveal the stomatal pore beneath, than those of the three older floret stages. In presecretory mature buds, the majority of modified stomata were open, however, and remained so throughout the stages of floret development until some (13%, table 1) were occluded (fig. 5E, *bottom*), sometimes by underlying parenchyma cells (fig. 5F). Most modified stomata remained open during the senescent phase (84%, table 1) even when adjacent epidermal cells had already collapsed (fig. 5D), and pore width remained large (table 1). Substomatal chambers beneath the modified stomata could be large (fig. 4F) or small (fig. 4D, 4E, *bottom left*).

Modified stomata contained more starch (fig. 3E, 3F; fig. 4E, 4G) than both nonspecialized epidermal cells and nectary parenchyma cells (fig. 3F; fig. 4F, 4G). Within the nectary, parenchyma cells were the dominant cell type and were small but variable in size (fig. 4F), ranging from ~10 to 20 μm.

The vasculature of the nectary consisted of phloem alone with no xylem progressing beyond the style or ovary into the nectary. Nectary phloem had two origins: vertical traces through phloem sieve tubes from the ovary (fig. 4B–4D) and horizontally oriented traces arising from phloem at the extreme base of the style (fig. 4H, 4J). Within the nectary, sieve tubes could branch and extend horizontally (fig. 3F, 3G), then continue vertically until they ended near or, in infrequent instances, at (fig. 3H) the pores of modified stomata. Sieve tubes were found adjacent to the outer epidermis of the nectary (fig. 4B, 4D), and both sieve elements and companion cells were in direct contact with epidermal cells (fig. 4F, 4H, 4K).

Dynamics of Nectar Secretion

Plants of *E. pallida* var. *angustifolia* from the three field sites were sampled for nectar, and these data were combined because the patterns were similar. Figure 6 illustrates the changes in mean nectar volume and nectar-sugar quantity per disk floret spanning the commencement of nectar accumulation
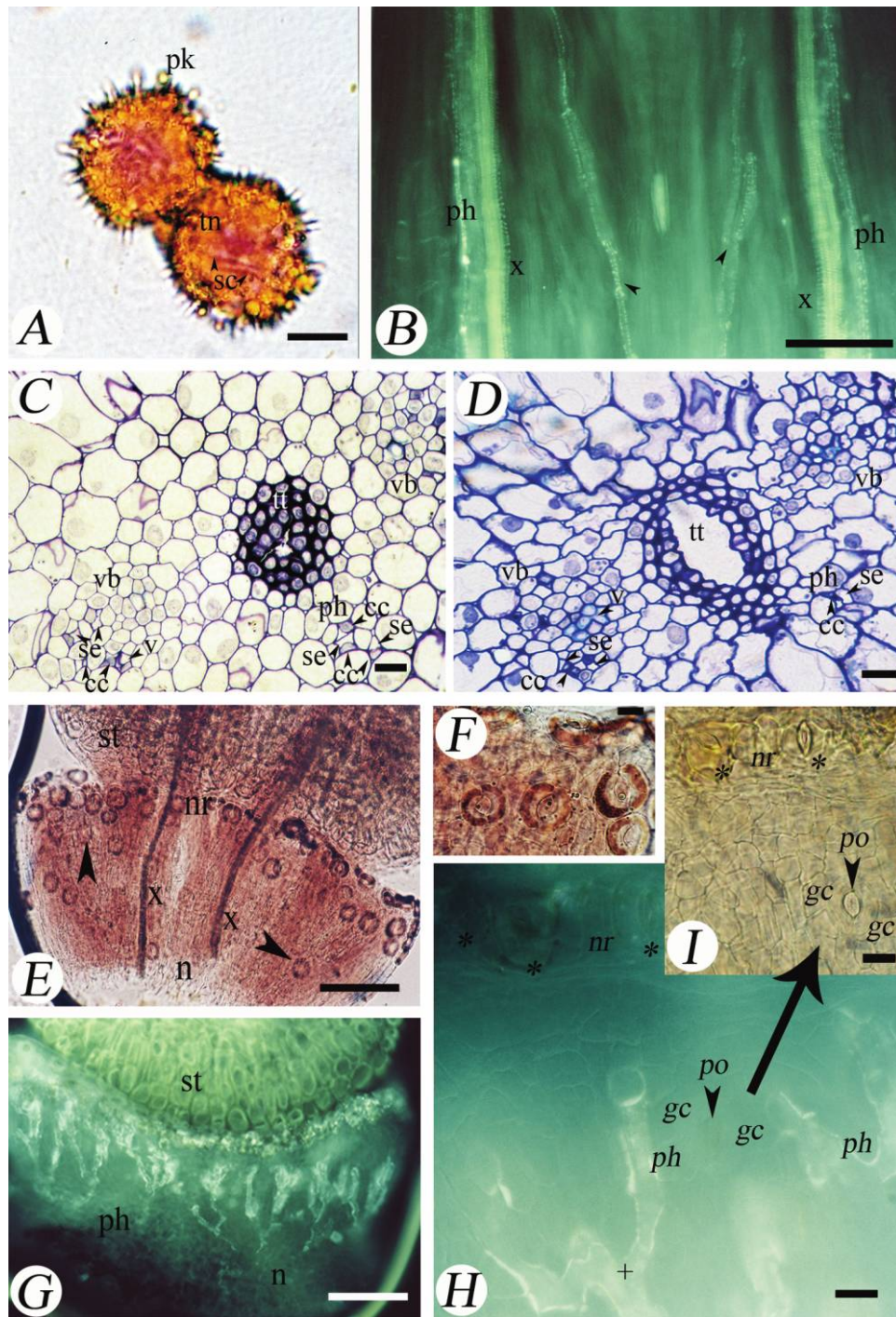
Fig. 3 Light and fluorescence micrographs of pollen, style, and nectary of disk florets. *A*, Trinucleate pollen grains of *Echinacea pallida* var. *angustifolia* stained with iron acetocarmine to show round tube nucleus (*tn*) and two laminar sperm cells (*sc*). Pollenkitt indicated by *pk*. Scale bar = 10 μm. *B*, Central portion of a longitudinally oriented style of *E. pallida* var. *angustifolia* stained with aniline blue, showing isolated sieve tubes (arrowheads) and the position of phloem (*ph*) and xylem (*x*) within the style's two vascular bundles. Scale bar = 50 μm. *C*, Transverse section through the style base of *Echinacea purpurea* in bud phase stained with toluidine blue, showing thick-walled cells of transmitting tissue (*tt*); isolated phloem (*ph*) with sieve element–companion cell complexes; and the sieve elements (*se*), companion cells (*cc*), and xylem vessel members (*v*) of the two vascular bundles (*vb*). Scale bar = 10 μm. *D*, Transverse section through style base of a pistillate-phase floret of *E. pallida* var. *angustifolia* stained with toluidine blue, showing central opening of the transmitting tract (*tt*); isolated phloem (*ph*) with sieve element–companion cell complexes; and the sieve elements (*se*), companion cells (*cc*), and xylem vessel members (*v*) of the two vascular bundles (*vb*). Scale bar = 10 μm. *E, F,* Nectaries of *E. pallida* var. *angustifolia* stained with I$_2$KI. *E,* Guard cells (arrowheads) containing starch grains along the rim (*nr*) and side walls of nectary (*n*). Note xylem (*x*) of the two vertically oriented vascular bundles entering style base (*st*). Scale bar = 50 μm. *F,* Abundant

(morning of the staminate phase SP) to the cessation of nectar production by the end of the third day of the pistillate phase (PP3), 4 d postanthesis.

Nectar Volume

At anthesis, disk florets of bagged inflorescences of *E. pallida* var. *angustifolia* in the staminate phase (SP Mo) held an average of 0.06 μL of nectar, which increased at midday to peak at 0.24 μL in the afternoon (fig. 6A). Nectar volume did not decrease significantly overnight, remaining high for the morning of the first pistillate day (PP1 Mo). Nectar volume decreased during the day of the first pistillate phase (fig. 6A). Up to this point, all sampled florets yielded sufficient nectar for refractometry. Mean nectar volume decreased significantly on the second day of the pistillate phase (PP2) and remained fairly constant during the day at just below 0.1 μL per disk floret (fig. 6A). By the morning of the second pistillate day (PP2), only 60% of sampled disk florets contained nectar, and at midday and afternoon samplings, only 42% of florets yielded nectar. Nectar volume declined to 0.01 μL during the third day of the pistillate phase, where most florets (84%) did not yield nectar. By the fourth day of the pistillate phase (PP4), nectar production had all but ceased, with only one of 62 florets yielding nectar.

Nectar Solute Concentration

Average nectar solute concentrations (refractometer measurements) rose throughout the staminate phase of disk florets from 40.4% (morning) to 54.4% (midday) and 63.0% (afternoon). However, during the first day of the pistillate phase (PP1), nectar solute concentrations remained relatively constant, averaging 63.6% $\pm$ 0.8%. Likewise, solute concentration averaged 62.6% $\pm$ 1.4% during the second pistillate day (PP2).

Nectar-Sugar Quantity

Mean nectar-sugar quantity per disk floret rose from 40.6 μg in the first hours after anthesis (SP Mo) to a peak of 191.7 μg by the afternoon of the staminate phase (SP Af) (fig. 6B). Due to the consistency in nectar solute concentration throughout floret phenology thereafter (above), nectar-sugar quantity per disk floret (fig. 6B) closely reflected the pattern of nectar volume (fig. 6A). The nectar-sugar quantity per floret remained high in the morning of PP1 but then decreased and remained relatively constant for the rest of that day (fig. 6B). The following day, nectar sugar per floret had fallen to 73.0 μg in the afternoon of PP2, and it decreased to 7.4 μg on the third day of stigma receptivity (PP3) before cessation of nectar production at PP4 (fig. 6B), with only a single floret yielding 0.63 μg from the total of 62 disk florets sampled.

Nectar-Carbohydrate Composition

Although the floral nectars of *E. pallida* var. *angustifolia* were dominated by hexoses, they varied in terms of which sugar predominated. The quantity of glucose (G) exceeded that of fructose (F) in six of nine samples. A small net reduction in nectar sucrose (S) content was observed as florets aged. For example, the G : F : S ratio of floral nectar sampled at the same time, but separately from disk florets of three adjacent whorls (SP, PP1, PP2) of plant 1, was 5.3 : 5.8 : 1, 3.8 : 3.8 : 1, and 6.8 : 6.8 : 1, respectively. However, plant 3 had proportionally more sucrose in PP2 (4.4 : 4.3 : 1) than in SP (12.8 : 9.9 : 1) or PP1 (15.8 : 16.5 : 1) florets.

Potential Honey Production

With a few assumptions, potential honey production from fields of *E. pallida* var. *angustifolia* can be assessed. Using the maximum amount of nectar sugar produced by a floret combined with the mean number of florets per capitulum, the total amount of nectar produced by one capitulum can be estimated. It was not determined whether nectar secretion occurred continuously throughout a single floret's phenology, so the maximum quantity of nectar sugar (191.7 μg) that occurred during the late staminate phase (SP Af; fig. 6B) could represent the total amount produced per floret; this approximation may be an underestimate. On the other hand, if nectar production continues after nectar withdrawal, the cumulative total nectar sugar collected throughout floret phenology (1100 μg; fig. 6B) may also be a worthy consideration. Multiplying these two masses per disk floret by an average of 202 florets per capitulum yields 38.7 and 222 mg of nectar sugar, respectively, available per inflorescence. Average planting densities of 21,780 plants per acre (53,800/ha) were determined in South Dakota (see "Discussion"). If inflorescences are present in the first year of planting, they are small and contain few florets, so nectar production will be low. In years 2 and 3 of growth, however, each plant should produce one average-sized inflorescence and, assuming complete survival of all plants from year 1 to year 2, it is estimated that one hectare should produce 2.1 kg (i.e., 53,800 plants $\times$ 38.7 mg nectar sugar per inflorescence) and 11.9 kg of nectar sugar, respectively. These values should increase in years 4 and 5, when each plant produces multiple inflorescences.

Discussion

Inflorescence Morphology

The capitulum of *Echinacea pallida* var. *angustifolia* is a highly modified aggregation of small florets, thus creating an illusion typical of many asteracean taxa, of one large, radially symmetric flower, presumably to attract pollinators (Weberling

starch within guard cells of several stomata. Scale bar = 10 μm. G, H, Nectaries of *E. pallida* var. *angustifolia* stained with aniline blue and viewed with fluorescence microscopy. G, Note abundance and location of ramifying sieve tubes (*ph*) of nectary (*n*). Style indicated by *st*. Scale bar = 50 μm. H, Nectary showing phloem (*ph*) sieve tubes branching horizontally (plus sign) before terminating vertically near pores (*po*) of modified stomata. Guard cells indicated by *gc*. Modified stomata (asterisks) on nectary rim (*nr*). Scale bar = 10 μm. I, Bright-field image of nectary from G indicating position of stomatal pore (*po*) and guard cells (*gc*) of modified stomate on nectary wall. Modified stomata (asterisks) on nectary rim (*nr*) correspond to those in *H*. Scale bar = 10 μm.
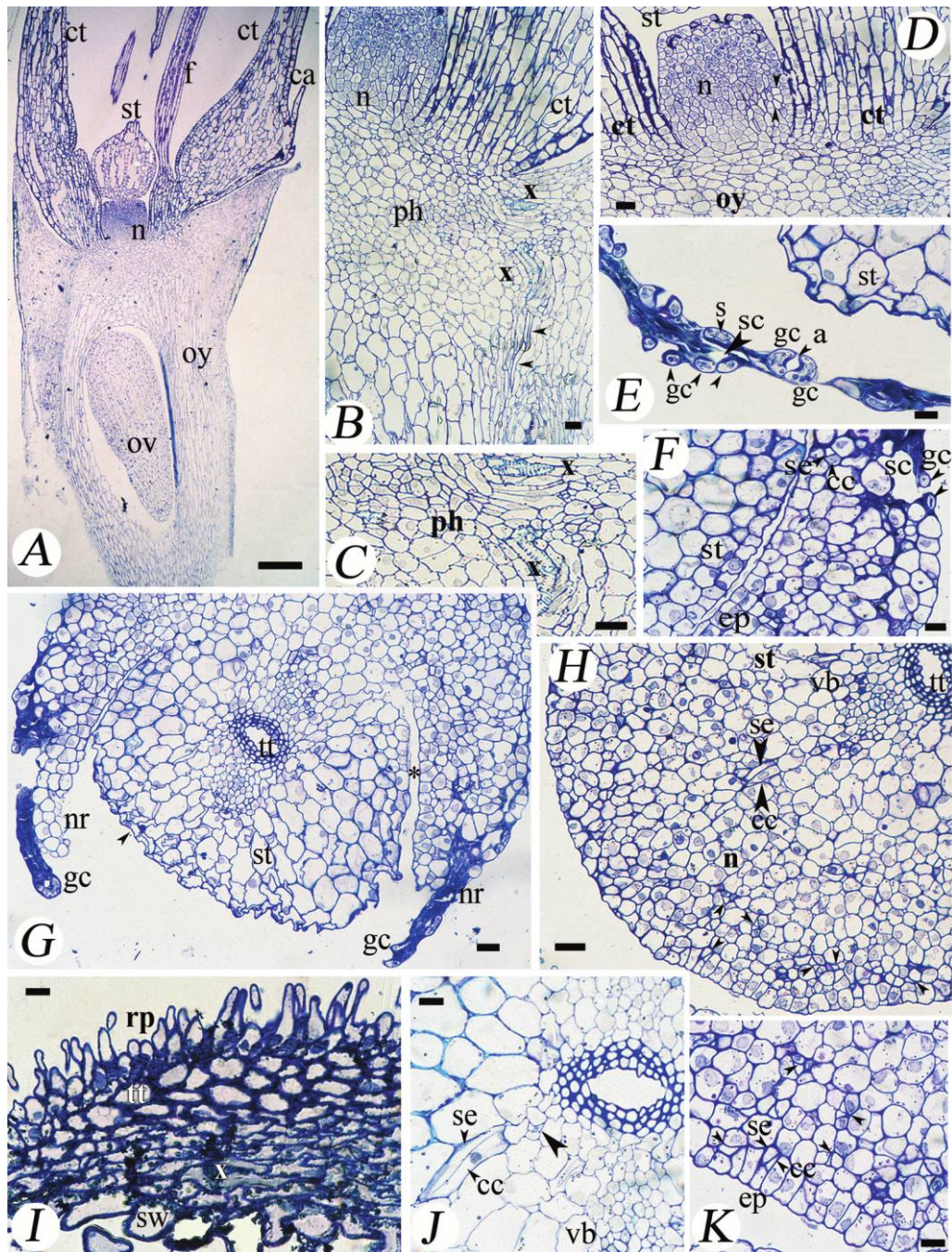
Fig. 4 Light micrographs of disk florets of *Echinacea pallida* var. *angustifolia*. *A–D*, Longitudinal sections through a staminate-phase floret. *E–K*, Cross sections through style base and nectary of a pistillate-stage floret. *A*, Tangential section showing nectary (*n*) below globular base of style (*st*), and ovule (*ov*) within inferior ovary (*oy*). Staminal filaments (*f*), corolla tube (*ct*), and reduced calyx (*ca*) also evident. Scale bar = 100 μm. *B*, Vascular trace extending from ovary base toward bases of corolla tube (*ct*) and nectary (*n*) with xylem vessels (*x*) and phloem sieve tubes (arrowheads) evident in longitudinal section. Phloem (*ph*) sieve elements and companion cells occur in cross section. *C*, Higher magnification of *B* showing the longitudinal vessels of xylem (*x*) and cross-sectional phloem (*ph*) in the ovary. *D*, Portion of nectary disk enclosed by base of corolla tube (*ct*) with phloem extending as a sieve tube through ovary (*oy*) and presumably connecting to phloem below nectary epidermis (arrowheads). Style indicated by *st*. *E*, Nectary rim with guard cells (*gc*) of modified stomata cut in various planes to show amyloplasts (*s*) within guard cells, substomatal chambers (*sc*), and undulating surface of style base (*st*). Stomatal aperture indicated by *a*. *F*, Large substomatal chamber (*sc*) continuous with aperture of a modified stomate. Note narrow interface between style base (*st*) and inner epidermis of nectary (*ep*) and presence of a phloem sieve element (*se*) and companion cell (*cc*) adjacent to inner epidermis. Guard cells indicated by *gc*. *G*, Oblique section of nectary showing intact guard cells (*gc*) amid deteriorating cells along rim (*nr*). At right (asterisk), cells of nectary base are contiguous with cells of style base (*st*). Transmitting tract indicated by *tt*. Note concave nature of exposed stylar epidermal cells (arrowhead), giving an

1989; Proctor et al. 1996). The common name, purple cone-flower, derives from the raised base of the inflorescence that bears the disk florets. The outer purple, petal-like ray florets are the first to reach anthesis and attract insects visually, but in this species, they are functionally sterile, lacking an androecium, entire gynoecium, or nectary. Each disk floret is subtended by a modified bract (palea) protruding beyond the corolla, and this stiff, spiny structure led to the generic name from the Greek *echinos*, a hedgehog (Kindscher 1989).

Structure and Phenology of Disk Florets

The membranous, scalelike pappus is the reduced form of the free, upper limbs of the sepals and apparently serves no functional purpose to disk florets of *E. pallida* var. *angustifolia* other than the calyx base fusing around the ovary, thus forming part of the indehiscent, mature fruit, as in several other asteracean taxa (Mani and Saravanan 1999). Without a hairlike pappus specialized for wind dispersal, such as in dandelion *Taraxacum officinale*, primary dispersal of the *Echinacea* achenes is reduced.

The fused corolla tubes of *E. pallida* var. *angustifolia* florets did not differ from the descriptions of McGregor (1968), who reported their lengths as 6–8 mm. The corolla's bell shape protects the androecium and upper gynoecium preanthesis, and its basal expansion postanthesis serves as a nectar reservoir. Filament bases also attach at the corolla base, common in the Asteraceae (Leins and Erbar 1987). At the stamen tips, the sterile anther apices may function in pollen portioning (Thiele 1988) and for protection of pollen shed within the anther tube from environmental damage, e.g., by excluding rain during the period when the style does not yet present pollen. At maturity, each bisporangiate anther of the tube contained microgametophytes that fell within the range (19–26 μm) reported for *E. pallida* var. *angustifolia* by McGregor (1968), ranking them small to intermediate within Asteraceae (Erdtman 1954). Pollen grains were echinate, a common feature of the Tubuliflorae (Erdtman 1954). The spines plus oily pollenkitt probably assist dispersal by helping grains adhere to body hairs of inflorescence-visiting insects. Before anther dehiscence, mature pollen grains of *E. pallida* var. *angustifolia* and *Echinacea purpurea* (Wist 2005) already contained a vegetative (tube) nucleus plus two sperm cells, evidently the first record of trinucleate pollen in *Echinacea*, typical of Asteraceae (Brewbaker 1967).

The gynoecium of each epigynous disk floret consisted of an inferior, unilocular ovary containing a single ovule. Atop the ovary, the style led to a bilobed stigma, conventional in Asteraceae (Mani and Saravanan 1999).

Stigmas of 17 asteracean genera were described as "dry," a feature common in taxa that employ a sporophytic self-incompatibility system to prevent self pollination (Heslop-Harrison and Shivanna 1977). The stigma of *E. pallida* var. *angustifolia* bifurcates into two lobes that reflex when receptive and may become moist, according to Leuszler et al. (1996). No evidence of a "wet" stigma was found in our observations of *E. pallida* var. *angustifolia*, but the stigmas of other Asteraceae may produce a small exudate (Knox 1973; Vithanage and Knox 1977; Elleman et al. 1992; Hiscock et al. 2002), and so technically are not dry (Elleman et al. 1992) but semidry (Hiscock et al. 2002). Stigmas of *Echinacea* may also share this semidry condition.

Stigmas of *E. pallida* var. *angustifolia* served a dual function during floret phenology. Initially, in the staminate phase, the unreceptive stigma with its adpressed lobes acted as a secondary pollen presenter (see Pacini 1996). The abaxial, nonreceptive surface of the stigma bore elongated trichomes that swept out pollen grains from the anther tube for presentation in the staminate phase, as the style lengthened and the staminal filaments contracted. Although pollen-catching hairs are absent on the stigma of some Asteraceae (Knox 1973), this type of active pollen presentation is typical (Ladd 1994; Pacini 1996). In addition, the stigma lobes reflexed during the disk floret's pistillate phase to expose their adaxial, receptive surfaces of unicellular papillae. Xenogamous pollen grains transferred by pollinators adhered to the surface of these papillae, where germination of pollen tubes initiated from pores on the grain surface. The single, elongating pollen tube from a compatible grain penetrated the stigma surface extracellularly, between receptive papillae, presumably where the cuticle is absent or thin (Elleman et al. 1992; Hiscock et al. 2002). Stigmas that remained free from cross-pollination for several days curled downward and contacted self pollen that may yet cling residually to the style and/or anther tips (fig. 2C). However, the effectiveness of this final, autogamous self-pollination process is unknown. The pistillate phase in *E. pallida* var. *angustifolia* eventually ends with floret senescence after 8–10 d, when the style shrivels and retracts into the corolla tube (fig. 1C; Wagenius 2004).

The style interior served as the conduit for pollen-tube growth of compatible grains from the stigma to the inferior ovary. A central, clearly delimited core of transmitting tract occurred between the style's two vascular bundles, extending upward into each stigmatic lobe. Transmitting tissue also occurs below the stigmatic papillae in *Cichorium intybus* (Erbar 2003), *Cynara cardunculus* (Duarte et al. 2006), and *Helianthus annuus* (Vithanage and Knox 1977). Passage of pollen tubes occurred extracellularly within the matrix surrounding the transmitting-tract cells, which in transverse section were roundish and small in diameter. Although these characteristics of the pollen-tube pathway in *E. pallida* var. *angustifolia* gener-

---

irregular surface. *H*, Horizontal phloem trace with sieve element (*se*) and companion cell (*cc*) extending externally from one of the two regular vascular bundles (*vb*) and traversing stylar tissue (*st*) toward nectary (*n*). Transmitting tract indicated by *tt*. Note phloem cells adjacent to epidermis and amid parenchyma cells of nectary (small arrowheads). *I*, Longitudinal section through tip of stigma lobe with a 1–4-celled layer of transmitting tract (*tt*) directly beneath papillae (*rp*) of receptive surface. Sweeping trichomes (*sw*) of pollen presenter and vessels of xylem trace (*x*). *J*, Horizontal sieve tube element (*se*) and companion cell (*cc*) supplying nectary and originating from phloem (arrowhead) external to vascular bundles (*vb*) of style. *K*, Higher magnification of outer epidermis of *H*. Sieve elements (*se*) and companion cells (*cc*) of vascular tissue next to outer epidermis (*ep*) of nectary. Other sieve element–companion cell complexes (arrowheads) evident amid nectary parenchyma. Scale bars for *B*–*K* = 10 μm.
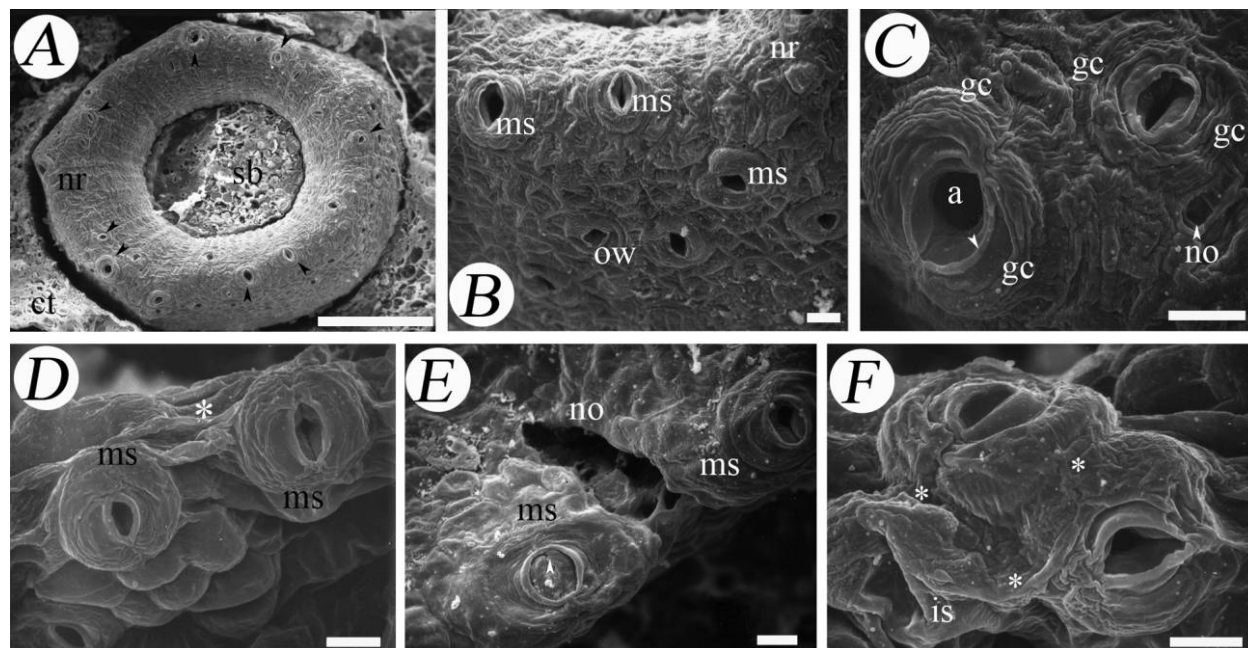
Fig. 5 SEMs showing characteristics of floral nectary of disk florets of *Echinacea pallida* var. *angustifolia*. *A*, Bud stage, showing modified stomata (arrowheads) on nectary rim (*nr*) and outer face of gland, which is surrounded by base of corolla tube (*ct*). Style base indicated by *sb*. *B*, Modified stomata (*ms*) on the rim (*nr*) and upper outside wall (*ow*) of nectary of a bud. *C*, Open modified stomata with raised guard cells (*gc*) typical on nectary rim, cuticular ledge (arrowhead) and stomatal aperture (*a*). Nonstomatal apical opening (*no*) visible in the epidermis. *D*, Modified stomata (*ms*) can remain open on senescent nectaries even after surrounding nonspecialized epidermal cells have collapsed (asterisk). *E*, The pore of this modified stomate (*ms*, lower left) on rim of a senescent nectary was occluded while another modified stomate (at top right) remained open. Large, nonstomatal apical opening (*no*) in epidermis. *F*, Three modified stomata with confluent guard cells (asterisk). Immature stomate indicated by *is*. All scale bars = 10 μm.

ally accorded with those of other asteracean styles (Vithanage and Knox 1977; Erbar 2003; Duarte et al. 2006), two structural features at the style base apparently are newly reported for the Asteraceae.

First, isolated traces of phloem alone, detectable by fluorescence microscopy (fig. 3*B*) and confirmed in transverse sections by LM to comprise sieve-tube elements and companion cells (fig. 3*C*, 3*D*), extend acropetally from the style base. These traces, extraneous from the two major vascular bundles running throughout the style's length, appear to continue vertically from some of the sieve tubes supplying the nectary. Their function is uncertain, but the propinquity of these spurious phloem traces to the transmitting tract infers a contribution of carbohydrate reserves that may assist pollen-tube growth.

Second, in the pistillate phase of disk florets of *E. pallida* var. *angustifolia*, the transmitting tract is centrally hollow. Below the style, this cavity eventually opens widely to the locule surrounding the ovule. The extracellular matrix and lacunate nature of the transmitting tissue provide opportunity for a low-resistance pathway for potentially many pollen tubes despite the theoretical need for just one. In the style of *E. purpurea*, however, the transmitting tract remained solid. Closely related taxa may have transmitting tracts that are hollow or solid throughout or that exhibit a transition between these two forms (Johri 1966).

Closely surrounding the tapered style base, the collar-shaped floral nectary of *E. pallida* var. *angustifolia* had a circular contour along its inner surface. Epidermes of these neighboring

Table 1

Dimensions (Mean ± SE) of the Floral Nectary of *Echinacea pallida* var. *angustifolia* and Developmental Stages and Dimensions of Its Modified Stomata at Four Phenological Phases of Disk Florets

| Phenological phase of floret | Nectary dimensions (μm) | | Modified stomata | | | | | | |
| | | | Number per developmental stage (%) | | | | Dimensions (μm) | | |
	Exterior width	Height	Total	Immature	Open	Occluded	Width	Length	Pore width
Mature bud	292 ± 32	164 ± 14	41.0 ± 3.0	8.5 ± 6.5 (21)	32.5 ± 9.5 (79)	.0 ± .0 (0)	20.0 ± .0	18.1 ± .9	5.5 ± .5
Staminate	422 ± 31	229 ± 28	35.7 ± 2.0	4.3 ± 1.9 (12)	29.0 ± 3.1 (81)	2.3 ± .3 (7)	21.0 ± 1.3	20.9 ± .8	4.0 ± .6
Pistillate	437 ± 17	171 ± 37	35.3 ± 2.0	1.7 ± .7 (5)	33.7 ± 2.2 (95)	.0 ± .0 (0)	23.6 ± .5	22.0 ± .9	6.6 ± 2.5
Senescent	552 ± 8.1	224 ± 15	40.0 ± 1.0	1.0 ± .6 (3)	33.7 ± 4.8 (84)	5.3 ± 4.3 (13)	27.6 ± 1.5	23.9 ± .7	7.0 ± .7

Note. Three florets are represented per phase. Stomatal measurements were taken from seven open stomata per nectary.
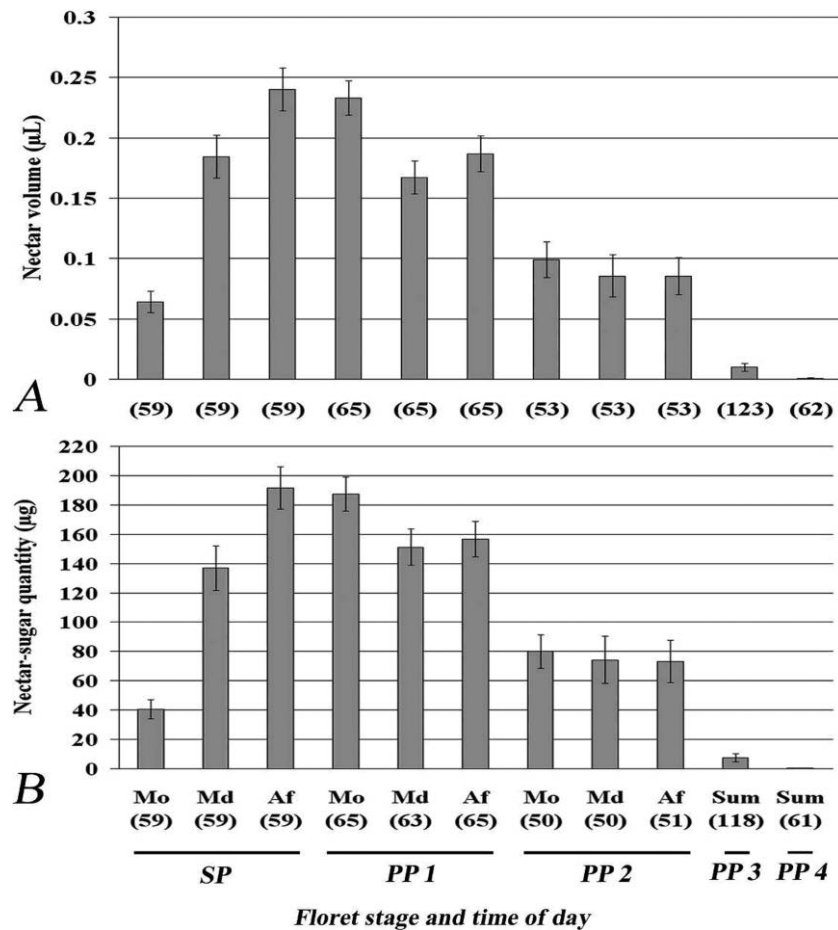
Fig. 6 Nectar characteristics of disk florets of *Echinacea pallida* var. *angustifolia*. *A*, Nectar volume (mean ± SE). *B*, Nectar-sugar quantity (mean ± SE). Morning (*Mo*), midday (*Md*), afternoon (*Af*). Staminate phase (*SP*); first day (PP1), second day (PP2), third day (PP3), and fourth day (PP4) of the pistillate phase. The numbers in parentheses represent, per floret stage and time of day, the total number of disk florets sampled (*A*) and all florets sampled minus those that yielded nectar but in insufficient quantities to have their nectar-solute concentrations register by refractometry (*B*).

floral organs showed clear signs of pressure exerted at this interface (fig. 4*F*, 4*G*). Consequently, the basal style surface was irregular, the outer periclinal walls of its epidermal cells often being depressed (fig. 4*D*). Similarly, to its exterior, the nectary was molded closely by the five petals of the corolla tube, yielding a pentagonal form as in *E. purpurea* (Wist and Davis 2006) and *Achillea millefolium* (Sulborska and Weryszko-Chmielewska 2006).

Overall, many other structural features were shared between the floral nectaries of *E. purpurea* (Wist and Davis 2006) and *E. pallida* var. *angustifolia*, though with quantitative differences. The latter was about 100 μm wider and 60 μm taller, and the average number of stomata (38) on its surface was about 10 higher. At any phenological stage, the floral nectary of each species could possess immature open and occluded stomatal pores (table 1). Pore occlusion is common (Thornburg et al. 2003; Wist and Davis 2006; Davis 2007; Nepi 2007), though the nature of the occluding material in this species is unknown. Open stomata surveyed on nectaries of *E. pallida* var. *angustifolia* had wider apertures, and substomatal chambers within the same gland could range greatly

in magnitude, the largest eliminating contact with the guard cells above. The evidence from these two studies of *Echinacea* does not lend itself to a regulatory role of nectar flow by the nectary stomata (Wist and Davis 2006), though pore-width closure noted in some asteracean nectaries has suggested regulatory capabilities of the stomata (Sammataro et al. 1985; Chatelet et al. 2005). Guard cells on the nectary of *E. pallida* var. *angustifolia* remained turgid and contained an abundance of starch, despite initial collapse of the postsecretory gland, like the demise of the annular nectary of *Glycine max* (Horner et al. 2003).

Apical openings near stomata on the rim occurred as gaps in the nectary epidermis. Like stomatal pores, these openings form a continuum with intercellular spaces and so provide an apoplastic pathway for nectar escape from the gland. Other floral nectaries bearing stomata (Davis and Gunning 1993; Vogel 1998; Davis 2007) and certain hydathodes (Mortlock 1952) possess similar gaps.

Like ∼32% of the Asteraceae studied to date (references in Wist and Davis 2006), the floral nectary of *E. pallida* var. *angustifolia* received a direct vascular supply consisting of

phloem alone. Sieve tubes from the ovary and style base innervated the nectary, with sieve-tube elements and companion cells extending directly beneath the epidermis on both the inner and outer nectary surfaces. Phloem below the epidermis has been illustrated in other floral nectaries of the Asteraceae (Frei 1955; Sammataro et al. 1985). As in *E. purpurea* (Wist and Davis 2006), nectary epidermal cells may participate in formation of the precursor cells of those sieve element–companion cell complexes. Some phloem traces also terminated close to stomatal pores on the nectary surfaces. In light of the hexose richness of the floral nectar of *E. pallida* var. *angustifolia*, if the phloem sap contains sucrose, raffinose, and myoinositol, as in other Asteraceae (Zimmermann and Ziegler 1975), sugar transformations evidently occur before nectar secretion. Carbohydrate-modifying enzymes could exist at this phloem-epidermis junction.

Nectar Characteristics and Potential Honey Production

Nectar solute concentration increased throughout the staminate phase, probably due to evaporation of water from standing nectar. A consistently high solute concentration throughout PP1 and PP2 may help maintain attractiveness of these receptive florets to nectar-gathering insects.

In bagged inflorescences in the field, average nectar volume per disk floret peaked at 0.24 μL during the afternoon of the day of anthesis, but it was 0.1 μL or less by the third day, when only 40%–60% of florets still yielded nectar. In *E. purpurea*, nectar volume was not maximal until midday of the day following anthesis, although the magnitude of its nectar volumes (Wist and Davis 2006) and that of sunflower (0.02–0.16 μL, Tepedino and Parker 1982; 0.04–0.32 μL, Vear et al. 1990) were comparable to these.

A reduction in nectar-sugar mass per disk floret, common during capitulum phenology within many asteracean taxa, occurred during the second day of anthesis in *E. pallida* var. *angustifolia*. By comparison, this decline happened about half a day sooner than in *E. purpurea* (Wist and Davis 2006) but half a day later than in *Cirsium kamtschaticum* (Nagamitsu et al. 2007). In the latter study, however, capitula were not bagged, so the potential effects of nectar withdrawal and pollination must be noted.

The maximum averages of 0.19 mg nectary sugar per disk floret at any interval sampled and an estimate of 0.4 mg total nectar carbohydrate collectible from each disk floret throughout a day are low to intermediate values when compared with other Asteraceae. For example, as reviewed by Crane et al. (1984), *Centaurea solstitialis* and *Centaurea cyanus* produced an average of 0.12 and 1.15 mg nectar sugar per floret each day, respectively, whereas *Taraxacum officinale* has a minimum of 0.43 mg nectar sugar per ligulate floret per day.

Like the floral nectar of most asteracean taxa studied (Percival 1961; Käpylä 1978), S, F, and G were present in nectar of three separate phenological stages (SP, PP1, PP2) of disk florets situated in consecutive rows within each capitulum. Asteracean nectar typically is hexose dominant (Baker and Baker 1983), but here the proportions of the three sugars varied with floret age. In plants 1 and 3, S predominated at PP1 and PP2, respectively. Moreover, the pattern of reduction in S content as disk florets progressed from staminate to pistillate stages on plants of *E. purpurea* in a growth chamber

was inverse (Wist and Davis 2006) to the pattern observed with *E. pallida* var. *angustifolia* in the field. Despite the variation, this ratio of hexoses to S evidently still maintains attractiveness of the aging disk florets to many Lepidoptera, Diptera, and the short- and long-tongued bees (Baker and Baker 1983) in the absence of pollen as a reward.

Nichol and Hall (1988) postulated that more than one route for nectar flow within the extrafloral nectary of *Ricinus communis* may account for differences observed in resultant nectar-carbohydrate composition. Here, variation in S content of nectar with disk-floret age might similarly reflect a differential origin or route of prenectar flow, such as a greater rate or proportion of S delivered by the sieve-tube elements to the nectary exterior than what might occur in the staminate phase. More research is required.

The potential honey production of 2.1–11.9 kg/ha from fields of *E. pallida* var. *angustifolia* were based on average densities of 53,800 plants/ha from South Dakota (Little 1999). These estimates of honey production are low compared with the literature reviewed by Crane et al. (1984) for *H. annuus* (46.8 kg/ha, compiled from 11 estimates) and *T. officinale* (up to 25 kg/ha). These data may explain why, in the relevant literature, *Echinacea* is not listed as an important plant for honey production in North America (Pellett 1923; Crane et al. 1984; Goltz 1988; Ayers and Harman 1992; Ayers 2005*a*, 2005*b*, 2006).

Visitor Rewards and Enhancement of Cross-Pollination

Whereas the ray florets of the perimeter serve to visually attract insect visitors to the capitulum of *E. pallida* var. *angustifolia*, in this species, these florets are sterile and nonrewarding. Thus, potential pollinators are well served by the landing platform provided by the inflorescence, where they are rewarded centrally by both nectar and pollen produced by the capitulum's disk florets. These are protandrous, a mechanism employed to reduce autogamy (Kevan 1997) in *Echinacea* and in general, throughout the Asteraceae (Erbar and Leins 1995; Pacini 1996).

The pollen : ovule ratios of 24,131 (*E. pallida* var. *angustifolia*) and 10,414 (*E. purpurea*) in disk florets are very high compared with *T. farfara* (1861; Wild et al. 2003), *C. intybus* (2451; Erbar and Enghofer 2001), and *Pectis multiflosculosa* (3973; Cruden 1977), and such values are generally indicative of xenogamous species (Cruden 1977). Within the Asteraceae, this difference (2.3) in pollen : ovule ratios between the two *Echinacea* spp. is intermediate to those in species pairs of *Adenocaulon* (1.1), *Pectis* (1.5), and *Bidens* (8.7) (Cruden 1977).

Although more expensive than nectar for the plant to produce as a reward (Simpson and Neff 1983), this copious surplus of oily pollen in *E. pallida* var. *angustifolia* provides a valuable source of nutrition for many visitors to staminate-phase florets. Dispensing clumps of pollen at the tip of the anther tubes into portions (Percival 1965) serves to extend its availability. Thereafter, pollen is still offered secondarily, in residual form, on the upper style and sweeping hairs on the abaxial surfaces of the stigma lobes (Erbar and Leins 1995; Pacini 1996).

Nectar, on the other hand, is produced in small volumes by disk florets. This pattern obliges many nectar-gathering in-

sects to visit many florets, and more than one capitulum, per foraging bout before they may become satiated. Accordingly, by carrying some of the bountiful pollen on its body, one individual may contribute to xenogamy of disk florets on several other plants of *E. pallida* var. *angustifolia*.

Throughout disk floret phenology, the quantity of nectar sugar approximated a normal distribution, centered at the afternoon of the staminate phase (SP) and the morning of the first day of the pistillate phase (PP1) in *E. pallida* var. *angustifolia*. Although highest throughout the day at PP1, when most of the pollen had already been offered, nectar-sugar mass decreased significantly in second-day pistillate florets (PP2), when approximately half of florets did not yield nectar. Very little nectar was still present in disk florets by the third (PP3) and fourth (PP4) days of stigmatic receptivity, much having been reclaimed by reabsorption, as in *E. purpurea* (Wist and Davis 2006). Without nectar or pollen as attractants, these florets will no longer be eagerly visited by insects. If these florets are not visited on their first day of receptivity, it is less likely that insects will intentionally visit the florets on days that follow. Thus, on the second and third days of receptivity, any transfer of cross pollen would need to occur passively by insects stepping on the still-receptive stigmas of older florets while visiting the first-day pistillate and staminate florets inward of them.

With its large surplus of pollen available to bees and beetles and the production of nectar with high solute concentration and high hexose composition common in a generalist pollination syndrome that includes flies, butterflies, and moths (Baker and Baker 1983), the phenological progression of reproductive events on the inflorescences of *E. pallida* var. *angustifolia* is indeed well adapted to "catering for the mass market" (Proctor et al. 1996) to enhance xenogamy by many visitors.

Acknowledgments

Literature Cited

Ayers GS 2005*a* The other side of beekeeping: asters in general. Am Bee J 145:729–733.

———— 2005*b* The other side of beekeeping: some colourful members of the aster family. Am Bee J 128:823–827.

———— 2006 More Asteraceae: a continuation of October 2005. Am Bee J 146:349–353.

Ayers GS, JR Harman 1992 Bee forage of North America and the potential for planting for bees: inventory and relative importance of nectar and pollen plants of North America. Pages 437–535 *in* JM Graham, ed. The hive and the honey bee. Dadant, Hamilton, IL.

Baker HG, I Baker 1983 Floral nectar sugar constituents in relation to pollinator type. Pages 117–141 *in* CE Jones, RJ Little, eds. Handbook of experimental pollination biology. Van Nostrand Reinhold, New York.

Belling J 1921 On counting chromosomes in pollen-mother cells. Am Nat 55:573–574.

Binns SE, BR Baum, JT Arnason 2000 A taxonomic revision of *Echinacea* (Asteraceae: Heliantheae). Syst Bot 27:610–632.

Brewbaker JL 1967 The distribution and phylogenetic significance of binucleate and trinucleate pollen grains in the angiosperms. Am J Bot 54:1069–1083.

Búrquez A, SA Corbet 1991 Do flowers reabsorb nectar? Funct Ecol 6:369–379.

Chatelet P, J Corre, N Delpierre, A Cottignies 2005 Illustration of nectar-producing structure of *Cynara cardunculus* L. var. *scolymus* (L.) Fiori. Acta Hortic 681:625–627.

Crane E, P Walker, R Day 1984 Directory of important world honey sources. International Bee Research Association, London.

Cruden RW 1977 Pollen-ovule ratios: a conservative indicator of breeding systems in flowering plants. Evolution 31:32–46.

Davis AR 2007 Informative epidermal features of various floral nectaries established as persistent, multicellular outgrowths. Pages 32–33 *in* 9th International Pollination Symposium on Plant-Pollinator Relationships. Iowa State University, Ames.

Davis AR, BES Gunning 1993 The modified stomata of the floral nectary of *Vicia faba* L. 3. Physiological aspects, including comparisons with foliar stomata. Bot Acta 106:241–253.

Davis AR, JD Pylatuik, JC Paradis, NH Low 1998 Nectar-carbohydrate production and composition vary in relation to nectary anatomy and location within individual flowers of several species of Brassicaceae. Planta 205:305–318.

Duarte P, R Figueiredo, S Pereira, J Pissarra 2006 Structural characterization of the stigma-style complex of *Cynara cardunculus* (Asteraceae) and immunolocalization of cardosins A and B during floral development. Can J Bot 84:737–749.

Elleman CJ, V Franklin-Tong, HG Dickinson 1992 Pollination in species with dry stigmas: the nature of the early stigmatic response and the pathway taken by pollen tubes. New Phytol 121:413–424.

Erbar C 2003 Pollen tube transmitting tissue: place of competition of male gametophytes. Int J Plant Sci 164(suppl):S265–S277.

Erbar C, J Enghofer 2001 Untersuchungen zum Reproduktionssystem der Wegwarte (*Cichorium intybus*, Asteraceae): Pollenportionierung, Narbenbelegung und Pollenschlauchkonkurrenz. Bot Jahrb Syst 123:179–208.

Erbar C, P Leins 1995 Portioned pollen release and the syndromes of secondary pollen presentation in the Campanulales-Asterales complex. Flora 190:323–338.

Erdtman G 1954 An introduction to pollen analysis. Ronald Press, New York.

Frei E 1955 Die Innervierung der floralen Nektarien dikotyler Pflanzenfamilien. Ber Schweiz Bot Ges 65:60–115.

Goltz L 1988 Honey and pollen plants. IX. Sunflowers and sunflower-like plants. Am Bee J 128:33–35.

Heslop-Harrison Y, KR Shivanna 1977 The receptive surface of the angiosperm stigma. Ann Bot 41:1233–1258.

Hiscock SJ, K Hoedemaekers, WE Friedman, HG Dickenson 2002 The stigma surface and pollen-stigma interactions in *Senecio squalidus* L. (Asteraceae) following cross (compatible) and self (incompatible) pollinations. Int J Plant Sci 163:1–16.

Horner HT, RA Healy, T Cervantes-Martinez, RG Palmer 2003 Floral nectary fine structure and development in *Glycine max* L. (Fabaceae). Int J Plant Sci 164:675–690.

Johansen DA 1940 Plant microtechnique. McGraw-Hill, New York.

Johri MM 1966 The stigma, style and pollen tube. III. Some taxa of the Amaryllidaceae. Phytomorphology 16:142–157.

Käpylä M 1978 Amount and type of nectar sugar in some wild flowers in Finland. Ann Bot Fenn 15:85–88.

Kevan PG 1997 Pollination biology and plant breeding systems. Pages 59–83 in KR Shivanna, VK Sawhney, eds. Pollen biotechnology for crop production and improvement. Cambridge University Press, New York.

Kindscher K 1989 Ethnobotany of purple coneflower (Echinacea angustifolia, Asteraceae) and other Echinacea species. Econ Bot 43:498–507.

Knox RB 1973 Pollen wall proteins: pollen-stigma interactions in ragweed and Cosmos (Compositae). J Cell Sci 12:421–443.

Ladd PG 1994 Pollen presenters in the flowering plants: form and function. Biol J Linn Soc 115:165–195.

Leins P, C Erbar 1987 Studien zur Blütenentwicklung an Compositen. Bot Jahrb Syst 108:381–401.

Leuszler HK, VJ Tepedino, DG Alston 1996 Reproductive biology of purple coneflower in southwestern North Dakota. Prairie Nat 28:91–102.

Little R 1999 Taming Echinacea angustifolia: research from SDSU and insights from a grower. http://biomicro.sdstate.edu/reesen/Echinacea/newsletter.htm.

Mani MS, JM Saravanan 1999 Pollination ecology and evolution in Compositae (Asteraceae). Science Publishers, Enfield, NH.

Martin FW 1959 Staining and observing pollen tubes in the style by means of fluorescence. Stain Technol 34:125–128.

McGregor RL 1968 The taxonomy of the genus Echinacea (Compositae). Univ Kans Sci Bull 48:113–142.

McKenna M, JD Thomson 1988 A technique for sampling and measuring small amounts of floral nectar. Ecology 69:1306–1307.

Mortlock C 1952 The structure and development of the hydathodes of Ranunculus fluitans Lam. New Phytol 51:129–138.

Nagamitsu T, T Kenta, K Inari, H Horita, K Goka, T Hiura 2007 Foraging interactions between native and exotic bumblebees: enclosure experiments using native flowering plants. J Insect Conserv 11:123–130.

Nepi M 2007 Nectary structure and ultrastructure. Pages 129–166 in SW Nicolson, M Nepi, E Pacini, eds. Nectaries and nectar. Springer, Dordrecht.

Nichol P, JL Hall 1988 Characteristics of nectar secretion by extrafloral nectaries of Ricinus communis. J Exp Bot 39:573–586.

O'Brien TP, ME McCully 1981 The study of plant structure: principles and selected methods. Termarcarphi, Melbourne.

Pacini E 1996 Tapetum types in the Compositae: forms and function. Pages 21–28 in DJN Hind, HJ Beentje, eds. Compositae: proceedings of the international Compositae conference, Kew, 1994. Royal Botanic Gardens, Kew.

Pellett FC 1923 American honey plants. 2nd ed. Dadant, Hamilton, IL.

Percival MS 1961 Types of nectar in angiosperms. New Phytol 60:235–281.

——— 1965 Floral biology. Pergamon, Oxford.

Proctor M, P Yeo, A Lack 1996 The natural history of pollination. Timber, Portland, OR.

Sammataro D, EH Erickson, MB Garment 1985 Ultrastructure of the sunflower nectary. J Apic Res 24:150–160.

Simpson B, J Neff 1983 Evolution and diversity of floral rewards. Pages 142–159 in C Jones, R Little, eds. Handbook of experimental pollination biology. Van Nostrand Reinhold, New York.

Sulborska A, E Weryszko-Chmielewska 2006 Morphology, anatomy and ultrastructure of yarrow (Achillea millefolium L.) floral nectaries. Acta Agrobot 59:17–28.

Tepedino VJ, FD Parker 1982 Interspecific differences in the relative importance of pollen and nectar to bee species foraging on sunflowers. Environ Entomol 11:246–250.

Thiele EM 1988 Bau und Funktion des Antheren-Griffel-Komplexes der Compositen. Dissertationes Botanicae, vol 117. Cramer, Berlin.

Thornburg RW, C Carter, A Powell, R Mittler, L. Rizhsky, HT Horner 2003 A major function of the tobacco floral nectary is defense against microbial attack. Plant Syst Evol 238:211–218.

Vear F, M Pham-Delegue, D Tourvielle de Labrouhe, R Marileau, Y Loublier, M le Métayer, P Douault, JP Philippon 1990 Genetical studies of nectar and pollen production in sunflower. Agronomie 10:219–231.

Vithanage HIMV, RB Knox 1977 Development and cytochemistry of stigma surface and response to self and foreign pollen in Helianthus annuus. Phytomorphology 27:168–179.

Vogel S 1998 Remarkable nectaries: structure, ecology, organophyletic perspectives. IV. Miscellaneous cases. Flora 193:225–248.

Wagenius S 2004 Style persistence, pollen limitation, and seed set in the common prairie plant Echinacea angustifolia (Asteraceae). Int J Plant Sci 165:595–603.

Weberling F 1989 Morphology of flowers and inflorescences. Cambridge University Press, Cambridge.

Wild J-D, E Mayer, G Gottsberger 2003 Pollination and reproduction of Tussilago farfara. Bot Jahrb Syst 124:273–285.

Wist TJ 2005 Pollination biology of Echinacea angustifolia and Echinacea purpurea (Asteraceae) in Saskatchewan. MS thesis. University of Saskatchewan, Saskatoon.

Wist TJ, AR Davis 2006 Floral nectar production and nectary anatomy and ultrastructure of Echinacea purpurea (Asteraceae). Ann Bot 97:177–193.

Zimmermann MH, H Ziegler 1975 List of sugars and sugar alcohols in sieve-tube exudates. Appendix III. Pages 480–503 in MH Zimmermann, JA Milburn, eds. Transport in plants. Vol 1. Phloem transport. Springer, Berlin.